OCTOBER 1981

PPPL-1841
UC-20G

HIGH-N COLLISIONLESS BALLOONING MODES IN AXISYMMETRIC TOROIDAL PLASMAS

BY

C.Z. CHENG

PLASMA PHYSICS LABORATORY

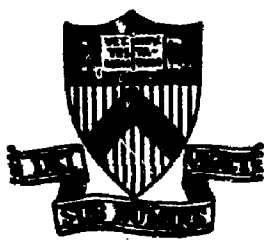

PRINCETON UNIVERSITY
PRINCETON, NEW JERSEY

This work was supported by the U.S. Department of Energy Contract No. DE-AC02-76-CHO 3073. Reproduction, translation, publication, use and disposal, in whole or in part, by or for the United States government is permitted.

High-n Collisionless Ballooning Modes in Axisymmetric Toroidal Plasmas

C. Z. Cheng

Plasma Physics Laboratory, Princeton University

Princeton, New Jersey 08544 USA

ABSTRACT

A collisionless kinetic ballooning mode equation, which includes the full ion finite Larmor radius (FLR), the magnetic drift, and the trapped electron effects, is derived and investigated for a large aspect ratio, circular flux surface equilibrium in the frequency regime, $\omega_{bi}, \omega_{ri} < \omega < \omega_{be}, \omega_{te}$. The finite Larmor radius effects can reduce the growth rate, but do not stabilize the ballooning modes due to the destabilizing influence of the ion magnetic drift resonances. It is, in general, incorrect to simulate the FLR effects by employing the often used FLR modified MHD model for $(k_\theta \rho_i)^2 \gtrsim 0.1$ and $\epsilon_n \gtrsim 0.1$, where $k_\theta \rho_i$ is the ion FLR parameter and $\epsilon_n = L_n/R$ measures the magnetic drift frequency. The trapped electrons have a stabilizing effect due to the reduction of the destabilizing circulating electron parallel current perturbation. For typical tokamak aspect ratio, the critical β can be improved by 40%.

I. INTRODUCTION

Ideal magnetohydrodynamic (MHD) theory predicts that in toroidal plasmas the ballooning modes can be driven unstable by the combined effects of the magnetic curvature and the pressure gradient. When β (the ratio of the plasma pressure to the magnetic pressure) lies between two critical values, say $\beta_1 < \beta < \beta_2$, unstable modes can develop and balloon in the bad curvature region [1-3]. One of the basic assumptions of the ideal MHD theory is that $\underset{\sim}{E} + \underset{\sim}{V} \times \underset{\sim}{B}/c = 0$. This assumption is not valid when kinetic effects such as finite larmor radius (FLR), magnetic drift and landau resonances, trapped particles and collisional effects are retained. Especially, these kinetic effects can be significant in the high-n limit (n is the toroidal mode number) and modify the critical beta [4-8].

It was generally believed that the FLR effects can reduce the growth rates and may yield total stabilization of the high-n MHD ballooning modes for arbitrary values of β. This conclusion is based on the investigation of the so-called FLR modified MHD ballooning mode equation [4-6] which has the same form as the ideal MHD ballooning mode equation, except ω^2 is replaced by $\omega(\omega - \omega_{*pi})$, where ω_{*pi} is the pressure driven ion diamagnetic drift frequency. Employing the high-n ballooning mode and WKB formalism [2,3] the FLR modified MHD ballooning mode equation is derived under two assumptions: (1) the perturbations have long perpendicular wavelength, $k_\perp \rho_i < 1$, and only the lowest order FLR contribution is retained, and (2) the ion magnetic drift frequency is small compared with the mode frequency, $\omega_{di} < \omega$, and is treated perturbatively without including drift resonances. In the ballooning mode formalism, the ion magnetic drift frequency ω_{di} and the perpendicular wavenumber $k_\perp$ are nonuniform along the magnetic field lines and can be written in the form, $\omega_{di} = \omega_0 + \omega_1\theta + \omega_2\theta^2$, where θ is the

extended poloidal angle and ω_0, ω_1, and ω_2 are periodic functions of θ with a period of 2π. Therefore, unless the eigenmode structure is well localized, the perturbative treatment of ω_{di}/ω and $k_\perp \rho_i$ can be invalid. Furthermore, the ion magnetic drift resonance can provide a destabilizing effect and modifies the stability analysis. In fact, it has been shown that there is no absolute FLR stabilization of the ballooning modes when full FLR and ion magnetic drift effects are retained [7,8].

The effect of trapped particles on the MHD ballooning mode has been found to be stabilizing by using a modified energy principle [4]. However, in these investigations, the trapped particle effects were not treated properly and the full finite Larmor radius and ion magnetic drift resonance effects were not retained. In this paper we will derive the high-n kinetic ballooning mode equation without making any assumptions on ω_{di}/ω and $k_\perp \rho_i$ [7-10]. Trapped particle effects will also be kept. The eigenmode equation in the collisionless limit have also been derived by various authors [9,10]. To assess the importance of these kinetic effects, we will compare the kinetic results with those from the FLR modified model and the ideal MHD model.

The paper is organized as follows. In Sec. II coordinate systems and MHD equilibria in an arbitrary toroidal geometry are described. In Sec. III the high-n ballooning mode and WKB formalism are applied to the gyrokinetic equations and Maxwell's equations and then the kinetic equations are expressed in these general coordinates. The eigenmode equations in the frequency range, where the frequency of the waves lies above the bounce and transmit frequencies of the ions but below those of the electrons, are derived in Sec. IV. The trapping effects are retained only for electrons and the collisional effects are neglected. The kinetic equations are then

shown to reduce to the FLR modified MHD ballooning model in the limits $k_\perp \rho_i \ll 1$ and $\omega_{di}/\omega \ll 1$. In the limiting case with $\eta_i = 0$, $\omega = \omega_{*i}$ and without trapped electron effects, the kinetic equation reduces to the ideal MHD ballooning mode equation at marginal stability. This means that the critical β is identical to the ideal MHD β_c and is independent of the ion Larmor radius and magnetic drift resonance effects. In Sec. V, we employ a large aspect ratio, low β, circular cross section model equilibrium used in a number of previous calculations [6,8,11-13] to study the stability of the ballooning modes. We then compare the results from the kinetic equations with those of the ideal MHD model and the FLR modified MHD model. The ion FLR and magnetic drift effects and the trapped electron effects are examined. No absolute ion FLR stabilization of the ballooning modes is found due to the ion magnetic drift resonances. The presence of trapped electrons is stabilizing because of the reduction of the destabilizing circulating electron parallel current perturbation. Finally, a summary of our paper is given in Sec. VI.

II. COORDINATES AND MHD EQUILIBRIA FOR TOROIDAL SYSTEMS

We will employ a coordinate system (ψ, θ, ζ) in which the field lines are straight and the magnetic field can be expressed by

$$\underset{\sim}{B} = \nabla\zeta \times \nabla\psi + q(\psi)\, \nabla\psi \times \nabla\theta \quad , \tag{1}$$

where $2\pi\psi$ is the poloidal flux between the magnetic axis and a ψ = constant surface, θ and ζ are the generalized poloidal and toroidal angles with a period of 2π, $q(\psi)$ is the safety factor and is a monotonic function of ψ only. In this coordinate system

$$\underset{\sim}{B}\cdot\nabla = J^{-1}\left[\left(\frac{\partial}{\partial\theta}\right)_{\psi,\zeta} + q(\psi)\left(\frac{\partial}{\partial\zeta}\right)_{\psi,\theta}\right] \quad , \tag{2}$$

where the Jacobian $J = (\nabla\psi \times \nabla\theta\cdot\nabla\zeta)^{-1}$. It is also advantageous to employ the coordinate system (ψ, θ, α), where $\alpha = \zeta - q(\psi)\theta$, so that $\underset{\sim}{B} = \nabla\alpha \times \nabla\psi$ and $\underset{\sim}{B}\cdot\nabla = J^{-1}(\partial/\partial\theta)_{\psi,\alpha}$.

Since the equilibrium magnetic field $\underset{\sim}{B}$ must satisfy the pressure balance condition,

$$\frac{1}{c}\,\underset{\sim}{j} \times \underset{\sim}{B} = \nabla p \quad , \tag{3}$$

where $p(\psi)$ is the equilibrium pressure, $\underset{\sim}{j} = (c/4\pi)\nabla \times \underset{\sim}{B}$ is the equilibrium current density, and c is the speed of light, the angles θ and ζ are not entirely arbitrary. From Eq. (3) we see that $\underset{\sim}{j}\cdot\nabla\psi = 0$ gives

$$\nabla\cdot[\nabla\psi \times (\nabla\alpha \times \nabla\psi)] = 0 \quad . \tag{4}$$

Equation (4) shows that θ can be arbitrarily specified, and ζ is determined by solving Eq. (4) or vice versa. Alternatively, we can specify the Jacobian and determine both θ and ζ. Although there is some analytic simplification by requiring J to be a function of ψ only as in the case of Hamada's coordinate system, computational experience [3] with high β equilibrium has shown that it is better to retain control over θ by allowing J to vary within a surface.

For the axisymmetric case, if we let ζ be the usual toroidal angle ϕ, then with the choice of Jacobian $J = x^2/f(\psi)$, where x is the distance from the axis of symmetry and $f(\psi)$ is determined by the periodicity

requirement, our coordinate system is essentially that of the PEST stability code [14]. If we instead choose $J = x/[f(\psi)|\nabla\psi|]$, we have equal arc lengths on the intersection of a magnetic surface with the ϕ = constant plane. This has been found to be optimal for numerically integrating the MHD ballooning mode equation along the extended θ direction [3]. By taking the $\nabla\psi$ component of Eq. (3), we obtain the Grad-Shafranov equation for the axisymmetric case

$$x^2[\nabla\cdot(\nabla\psi/x^2) + 4\pi(\partial p/\partial\psi)] + g(\partial g/\partial\psi) = 0 \quad , \tag{5}$$

where

$$g(\psi) = -q(\psi)[1 + \frac{\partial\delta}{\partial\theta}]\frac{x^2}{J} \quad , \quad \zeta = \phi - q(\psi)\delta(\psi, \theta) \quad .$$

Note that $\delta(\psi, \theta)$ is determined by Eq. (4) by arbitrarily specifying G. If we specify $p(\psi)$, $q(\psi)$, and J, then ψ is determined by Eq. (5).

For axisymmetric toroidal plasmas, the lowest order (in ρ/L, ρ is the particle Larmor radius and L is the macroscopic scale length) equilibrium distribution function is roughly a local isotropic Maxwellian distribution, $F_M(E, \psi) = N_0(\psi)[m/2\pi T(\psi)]^{3/2} \exp[-mE/T(\psi)]$ where $E = v^2/2$. The macroscopic pressure is given by $p(\psi) = N(\psi)T(\psi)$, and therefore in kinetic description we have one more degree of freedom in determining $p(\psi)$.

III. GYROKINETIC AND MAXWELL'S EQUATIONS IN HIGH-n BALLOONING MODE AND WKB FORMALISM

Low frequency perturbations, such as drift waves and ballooning modes

in toroidal plasmas, have very short wavelengths perpendicular to the sheared magnetic field $\underset{\sim}{B}$ in comparison with the parallel wavelength, $k_{\parallel}/k_{\perp} \ll 1$. However, in solving eigenmode equations, $L(\psi, \theta, \zeta, \omega)\Phi(\psi, \theta, \zeta) = 0$, a formal WKB type expansion in lowest order in $k_{\parallel}/k_{\perp}$ would lead to an aperiodic lowest order eigenfunction in θ since the field lines do not close on themselves on a magnetic surface whose safety factor, q, is irrational. In order to solve the problem of satisfying the periodic constraint in θ the ballooning representation is introduced by representing the eigen-function as an infinite sum of aperiodic functions [2,3] which add up to give a periodic function; i.e.,

$$\Phi(\psi, \theta, \zeta) = \sum_{p=-\infty}^{\infty} \hat{\Phi}(\psi, \theta-2\pi p, \zeta) \quad , \tag{5}$$

where $\hat{\Phi}$ extends from $-\infty$ to ∞ in θ. To ensure convergence of this sum, $\hat{\Phi}$ must vanish sufficiently fast as $|\theta| \to \infty$. Since the linear operator $L(\psi, \theta, \zeta, \omega)$ is periodic in θ, the aperiodic components can be assumed to obey the original eigenmode equations. Thus, the problem is equivalent to solving the eigenmode equation over an infinite range in θ with no periodicity constraint; i.e.,

$$L(\psi, \theta, \zeta, \omega)\hat{\Phi}(\psi, \theta, \zeta) = 0 \quad . \tag{6}$$

Since the perturbations of interest are locally flute like, we use $\varepsilon \equiv 1/n \sim O(k_{\parallel}/k_{\perp})$ as an expansion parameter to develop an asymptotic solution of Eq. (6). The solution of Eq. (6) can be expressed by the eikonal representation,

$$\hat{\Phi} = \hat{\phi}(\psi, \theta, \varepsilon) \exp[iS(\alpha, \psi)/\varepsilon] \quad , \tag{7}$$

where $S(\alpha, \psi)$ describes the rapid cross-field variations and $\hat{\phi}$ the slow variations along the field lines on the equilibrium length scale. Therefore, $\underset{\sim}{B}\cdot\nabla S = 0$, i.e., $\partial S/\partial\theta = 0$. In the axisymmetric case, S is separable and can be expressed as

$$S(\alpha, \psi) = \alpha + \int \theta_k(\psi)\, dq \quad , \tag{8}$$

where θ_k is to be determined by a higher order radially nonlocal analysis [2,3]. By our choice of straight field line coordinates, we have avoided the need for an eikonal description of the fast θ-dependence [2,3].

Since the ε dependence of L is explicit, we can expand L in powers of ε: $L = L^{(0)} + \varepsilon L^{(1)} + \ldots$, where $L^{(0)}$ is an operator only in θ space. Expanding $\hat{\phi}$ and ω in similar series and demanding that Eq. (6) be satisfied order by order gives, at the lowest order,

$$L^{(0)}(\psi, \theta\text{-}\theta_k, \omega^{(0)}, n)\hat{\phi}^{(0)} = 0 \quad . \tag{9}$$

This is a one-dimensional differential-integral equation for a given ψ, θ_k, and n. With proper boundary conditions, it defines an eigenvalue problem and gives the lowest order eigenvalue $\omega^{(0)} = \omega^{(0)}(\psi, \theta_k, n)$. The fact that θ_k occurs in Eq. (9) only in the combination $(\theta-\theta_k)$ implies that $\omega^{(0)}$ is a periodic function of θ_k. Therefore, within the WKB approximation the spectrum of the flute-like modes are infinitely degenerate, corresponding to each component of the infinite sum in the ballooning representation, Eq. (5). In the following, we will choose $\theta_k = 0$ so that the perturbations are

centered at the outside of the torus. This choice of θ_k is made because from computational experience the maximum growth rate occurs at $\theta_k = 2\pi p$ ($p = 0 \pm 1, \ldots$) for up-down symmetric equilibria [2-8].

Applying this high-n ballooning mode and WKB formalism, the lowest order linearized gyrokinetic equation is given by

$$\left(\omega + i\,\frac{v_\parallel}{BJ}\frac{\partial}{\partial\theta} - \omega_d\right)g = (\omega-\omega_*^T)\frac{eF_M}{T}\left(\phi J_0 - \frac{1}{c}\,v_\parallel A_\parallel J_0 - i\,\frac{v_\perp A_\perp}{c}\,J_1\right) \quad , \tag{10}$$

where the perturbed distribution function g, electrostatic potential ϕ and vector potentials $A_\parallel$, $A_\perp$ account for the slow variations along the field lines. In Eq. (10) $A_\parallel = \underset{\sim}{A}\cdot\hat{e}_B$, $A_\perp = \hat{e}_3\cdot\underset{\sim}{A}$, $\hat{e}_3 = \hat{e}_B\times\nabla S/|\nabla S|$, $\hat{e}_B = \underset{\sim}{B}/B$, with $\omega_d = \omega_B(\hat{v}_\perp^2/2) + \omega_\kappa\hat{v}_\parallel^2$, $\omega_\kappa = (2ncT/eB)\hat{e}_B\times(\hat{e}_B\cdot\nabla\hat{e}_B)\cdot\nabla S$, and $\omega_B = (2ncT/eB^2)\hat{e}_B\times\nabla B\cdot\nabla S$. From the MHD equilibrium condition, Eq. (3), $\omega_B = \omega_\kappa - \omega_*[\beta_e(1+\eta_e) + \beta_i(1+\eta_i)]$, with $\eta = d\ell nT/d\ell nN$, $\beta_{e,i} = 8\pi NT_{e,i}/B^2$, $\hat{v} = v/v_{th}$, $v_{th}^2 = 2T/m$, $\omega_* = (ncT/eB)\hat{e}_B\times\nabla\ell nN\cdot\nabla S$, and $\omega_*^T = \omega_*[1 + \eta(\hat{v}^2 - 3/2)]$. Finally, $J_{0,1} = J_{0,1}(k_\perp v_\perp/\Omega)$ are the Bessel functions of the first kind with orders zero and one, respectively, and $\underset{\sim}{k}_\perp = n\nabla S$, $\Omega = eB/mc$. Note that the superscripts of g, ϕ, $A_\parallel$, $A_\perp$, and ω are neglected, because we will only deal with this lowest order equation in the remainder of the paper.

The linearized, one-dimensional gyrokinetic equations are coupled by the quasineutrality condition and Ampere's law to form the basic set of integro-differential equations governing the eigenmodes of the system. Within the WKB ordering, the quasineutrality condition can be expressed as

$$\sum_{e,i} e\int d^3v\left(gJ_0 + \frac{e\phi}{m}\frac{\partial F_M}{\partial E}\right) = 0 \quad , \tag{11}$$

with the summation being over the particle species. Ampere's law is given by

$$(n\nabla S)^2(\hat{e}_B A_\parallel + \hat{e}_3 A_\perp) = \frac{4\pi}{c} \sum_{e,i} e \int d^3v \, (\hat{e}_B v_\parallel J_0 - \hat{e}_3 i v_\perp J_1) g \quad . \tag{12}$$

IV. HIGH-n BALLOONING MODE EQUATIONS

Since the ballooning mode frequency ω near marginal stability is of the same order as the ion diamagnetic drift frequency ω_{*i}, we expect, for high-n modes, ω to lie in the frequency regime: $\omega_{bi}, \omega_{ti} < \omega < \omega_{be}, \omega_{te}$, where $\omega_{ti}(\omega_{bi})$ and $\omega_{te}(\omega_{be})$ are the average ion and electron transit (bounce) frequencies, respectively. To ensure $\omega > \omega_{ti}$, we require $n > (\varepsilon_o L_n/q^2\rho_i)$, where $\varepsilon_o = r/R$ is the inverse aspect ratio of the torus, L_n is the density scale length, ρ_i is the ion Larmor radius, and q is the safety factor. $\omega < \omega_{be}$ implies that $n < (\varepsilon_o^{3/2} L_n/q^2\rho_e)$, where ρ_e is the electron Larmor radius, and this condition is easier to be satisfied for the wavelengths of interest. On the other hand, we require $n < (\varepsilon_o^{3/2} L_n/q^2\rho_i)$ for low frequency modes with $\omega < \omega_{bi}$. For such low values of n, it may be necessary to carry out the next order WKB expansion in $1/n$ in order to obtain meaningful eigen solutions. Therefore, we should limit ourselves to high-n modes with $\omega_{bi}, \omega_{ti} < \omega < \omega_{be}, \omega_{te}$.

For $\omega > \omega_{ti}$, the solution of Eq. (10) for ions is given by

$$g_i = \frac{G_i}{\omega - \omega_{di}} + O\left(\frac{\omega_{ti}}{\omega}\right) \quad , \tag{13}$$

where

$$G_j = (\omega-\omega_{*i}^T)\frac{eF_M}{T_i}\left(\phi J_0 - \frac{1}{c}v_\parallel A_\parallel J_0 - i\frac{v_\perp A_\perp}{c}J_1\right)_i \quad .$$

The general solution for circulating electrons with the boundary conditions $g_\sigma(\theta) \to 0$ as $\theta \to \pm\infty$ is given by

$$g_\sigma(\theta) = i\sigma \int_{-\sigma\infty}^{\theta} d\theta' \, \chi_\sigma \exp(-i\sigma I_\theta^{\theta'}) \quad , \tag{14}$$

where

$$\chi_\sigma = \chi_\phi - \sigma\chi_A \quad ,$$

$$\chi_\phi = \frac{B}{|v_\parallel|}(\omega-\omega_{*e}^T)\frac{eF_M}{T_e}\left(\phi J_{0e} - \frac{iv_\perp}{c}A_\perp J_{1e}\right) \quad ,$$

$$\chi_A = B(\omega-\omega_{*e}^T)\frac{eF_M}{T_e}\frac{A_\parallel J_{0e}}{c} \quad ,$$

$$I_{\theta_1}^{\theta_2} = \int_{\theta_1}^{\theta_2} d\theta \, \frac{B}{|v_\parallel|}(\omega-\omega_{de}) \quad ,$$

and $\sigma = \pm$ refers to the sign of $v_\parallel$ for particles in question. Note that $I_{\theta_1}^{\theta_2}$ is of the order of ω/ω_{te} and Eq. (14) can be reduced to

$$g_c = \frac{1}{2}(g_+ + g_-) = -\left(\frac{\omega-\omega_{*e}^T}{\omega}\right)\frac{eF_M}{T_e}\psi_\parallel + O\left(\frac{\omega}{\omega_{te}}\right) \quad , \tag{15}$$

where

$$\psi_\parallel = \frac{i\omega}{2c}\left(\int_{-\infty}^{\theta} d\theta' \; JBA_\parallel J_{0e} - \int_{\theta}^{\infty} d\theta' \; JBA_\parallel J_{0e}\right) \quad . \tag{16}$$

For trapped electrons, the boundary conditions at the turning points are $g_+(\theta_1) = g_-(\theta_1)$ and $g_+(\theta_2) = g_-(\theta_2)$, where θ_1 and θ_2 refer to the nearest turning points with $\theta_1 \le \theta \le \theta_2$. Note that there are infinite pairs of turning points in the extended θ space for trapped particles. The general solution for trapped electrons is

$$g_\sigma(\theta) = \exp(i\sigma I_{\theta_1}^{\theta})(-2\sin I_{\theta_1}^{\theta_2})^{-1} \int_{\theta_1}^{\theta_2} d\theta' \left[\chi_- \exp(iI_{\theta_2}^{\theta'}) + \chi_+ \exp(-iI_{\theta_2}^{\theta'})\right]$$

$$+ i\sigma \int_{\theta_1}^{\theta} d\theta' \, \chi_\sigma \exp(-i\sigma I_{\theta}^{\theta'}) \quad . \tag{17}$$

Since $I_{\theta_1}^{\theta_2}$ is of the order of ω/ω_{be} for trapped electrons, Eq. (17) reduces to

$$g_\sigma(\theta) = (I_{\theta_2}^{\theta_1})^{-1} \int_{\theta_1}^{\theta_2} d\theta' \, (\chi_\phi + iI_{\theta_2}^{\theta'}\chi_A) - i \int_{\theta_1}^{\theta} d\theta' \chi_A + O(\frac{\omega}{\omega_{be}}) \quad , \tag{18}$$

and the total nonadiabatic trapped electron distribution function is

$$g_t = \frac{1}{2}(g_+ + g_-)$$

$$= (I_{\theta_2}^{\theta_1})^{-1} \int_{\theta_1}^{\theta_2} d\theta' \left[\chi_\phi + i\chi_A (I_{\theta_1}^{\theta'} + I_{\theta_2}^{\theta'})/2\right] - \frac{i}{2}\left(\int_{\theta_1}^{\theta} d\theta' \, \chi_A + \int_{\theta_2}^{\theta} d\theta' \, \chi_A\right)$$

$$+ O(\omega/\omega_{be}) \quad . \tag{19}$$

Let

$$\langle R \rangle \equiv \int_{\theta_1}^{\theta_2} d\theta \, (B/|v_\parallel|) \, R \quad / \quad \int_{\theta_1}^{\theta_2} d\theta \, (B/|v_\parallel|) \quad , \tag{20}$$

and

$$\hat{\phi}_\parallel = \frac{i\omega}{\Sigma c} \left(\int_{\theta_1}^{\theta} d\theta' \, \frac{BA_\parallel J_{0e}}{c} - \int_{\theta}^{\theta_2} d\theta' \, \frac{BA_\parallel J_{0e}}{c} \right) \quad . \tag{21}$$

Then, g_t can be written as

$$g_t = -\left(\frac{eF_M}{T_e}\right)\left[\frac{\omega-\omega_{*e}^T}{\omega} \hat{\phi}_\parallel + \frac{\omega-\omega_{*e}^T}{\omega-\langle\omega_{de}\rangle} \langle \phi J_{0e} + \frac{iv_\perp A_\perp J_{1e}}{c} - \left(\frac{\omega-\omega_{de}}{\omega}\right)\hat{\phi}_\parallel \rangle \right] + O\left(\frac{\omega}{\omega_{be}}\right) \quad . \tag{22}$$

If we further assume that

$$\langle \phi J_{0e} + \frac{iv_\perp A_\perp J_{1e}}{c} - \left(\frac{\omega-\omega_{de}}{\omega}\right)\hat{\phi}_\parallel \rangle \approx \phi J_{0e} + \frac{iv_\perp A_\perp J_{1e}}{c} - \left(\frac{\omega-\langle\omega_{de}\rangle}{\omega}\right)\hat{\phi}_\parallel \quad ,$$

then

$$g_t = -\left(\frac{eF_M}{T_e}\right)\left[\frac{\omega-\omega_{*e}^T}{\omega-\langle\omega_{de}\rangle} \left(\phi J_{0e} + \frac{iv_\perp A_\perp J_{1e}}{c}\right)\right] + O\left(\frac{\omega}{\omega_{be}}\right) \quad . \tag{23}$$

The total electron nonadiabatic distribution is given by $g = g_c + g_t$.

Since $\omega < \omega_{he}, \omega_{te}$, we must retain the $O(\omega/\omega_{be})$ or $O(\omega/\omega_{te})$ contribution of the electron distribution function in order to obtain the electron parallel current perturbation $j_\parallel$. However, it is often convenient to obtain $j_\parallel$ by taking the moment of the gyrokinetic equation, Eq. (10). Noting that

$$\int d^3v \, \frac{v_\parallel}{B} \frac{\partial}{\partial\theta} g = -\frac{1}{B} \frac{\partial}{\partial\theta} \left(\frac{1}{B} \int d^3v \, v_\parallel g \right) \quad , \tag{24}$$

because $\int d^3v = \sum_\sigma \sqrt{2}\,\pi \int_0^\infty dE \frac{B}{E^{1/2}} \frac{d\mu}{|v_\parallel|}$ and $\mu = v_\perp^2/2B$. Then from Eq. (19), we have, by setting $J_{0e} \equiv 1$,

$$\frac{1}{\partial\theta}\frac{\partial}{\partial\theta}\left(\frac{1}{B}\int d^3v\, v_\parallel g\right) = i\int(\omega-\omega_{*_e})g\, d^3v + i\int(\omega-\omega_{*e}^T)\frac{eF_M}{T_e}\left(\phi+\frac{iv_\perp A_\perp J_{1e}}{c}\right)d^3v \quad . \tag{25}$$

Substitution of Eqs. (13), (15), and (23) into the quasineutrality condition given by Eq. (11) yields

$$(1+\tau-T_1-I_1)\,\phi - (T_2+I_2)\,\psi_\perp - U_1\psi_\parallel = 0 \quad , \tag{26}$$

where

$$I_1 = \tau\int\left(\frac{\omega-\omega_{*i}^T}{\omega-\omega_{di}}\right)F_M J_{0i}^2\, d^3v \quad ,$$

$$I_2 = \tau\int\left(\frac{\omega-\omega_{*i}^T}{\omega-\omega_{di}}\right)F_M\, J_{0i}J_{1i}\left(\frac{v_\perp}{c}\right)d^3v \quad ,$$

$$T_1 = \int_T \left(\frac{\omega-\omega_{*e}^T}{\omega-\langle\omega_{de}\rangle}\right)F_M\, d^3v \quad ,$$

$$T_2 = \int_T \left(\frac{\omega-\omega_{*e}^T}{\omega-\langle\omega_{de}\rangle}\right)F_M\, J_{1e}\left(\frac{v_\perp}{c}\right)d^3v \quad ,$$

$$U_1 = \int_U \left(\frac{\omega-\omega_{*e}^T}{\omega}\right)F_M\, d^3v \quad ,$$

$\Phi_\perp = iA_\perp$, $\tau = T_e/T_i$, and T and U refer to integration over trapped and untrapped particles, respectively.

The perpendicular Ampere's law, Eq. (12), reduces to

$$(T_2 + I_2)\phi + (k_\perp^2\lambda_e^2 + T_3 + I_3)\phi_\perp + U_2\phi_\parallel = 0 \quad , \tag{27}$$

where

$$k_\perp^2\lambda_e^2 = (n\nabla S)^2 T_e/4\pi N_e^2 \quad ,$$

$$I_3 = \tau \int_T^{} \left(\frac{\omega-\omega_{*i}}{\omega-\omega_{di}}\right) F_M \left(\frac{v_\perp}{c} J_{1i}\right)^2 d^3v \quad ,$$

$$T_3 = \int_T^{} \left(\frac{\omega-\omega_{*e}}{\omega-\langle\omega_{de}\rangle}\right) F_M \left(\frac{v_\perp}{c} J_{1e}\right)^2 d^3v \quad ,$$

$$U_2 = \int_U^{} \left(\frac{\omega-\omega_{*e}}{\omega}\right) F_M \frac{v_\perp}{c} J_{1e}\, d^3v \quad .$$

From Eqs. (13), (15), (23), and (25), the parallel Ampere's law, Eq. (12), can be written as

$$\frac{1}{\partial\theta}\frac{\partial}{\partial\theta}\frac{(n\nabla S)^2}{B^2}\frac{\partial}{\partial\theta}\phi_\parallel = \frac{4\pi N e^2\omega^2}{T_e c^2}\left\{U_1(\phi - \phi_\parallel) + U_3\phi_\parallel + T_4\phi + (U_4 + T_5)\phi_\perp\right\} \quad , \tag{28}$$

where

$$U_3 = \int_U \left(\frac{\omega_{de}}{\omega}\right)\left(\frac{\omega-\omega_{*e}^T}{\omega}\right)F_M \, d^3v \quad ,$$

$$T_4 = \int_T \left(\frac{\omega_{de}-\langle\omega_{de}\rangle}{\omega-\langle\omega_{de}\rangle}\right)\left(\frac{\omega-\omega_{*e}^T}{\omega}\right)F_M \, d^3v \quad ,$$

$$T_5 = \int_T \left(\frac{\omega_{de}-\langle\omega_{de}\rangle}{\omega-\langle\omega_{de}\rangle}\right)\left(\frac{\omega-\omega_{*e}^T}{\omega}\right)F_M \frac{v_\perp}{c} J_{1e} \, d^3v \quad .$$

Note that the parallel current perturbation is due to electrons because the ion contribution is of the order of $(\omega_{ti}/\omega)^2$ smaller and is neglected.

In order to carry out the velocity space integration of the electron terms, we will employ as our velocity space coordinates, v, λ, and σ, where $\lambda = h(\theta)v_\perp^2/v^2$, $h(\theta) = B_o/B(\theta)$, and $B_o^{-1} = \int_{-\pi}^{\pi} d\theta/B(\theta)$. In terms of these variables, we have

$$\int d^3v = \sum_\sigma \pi \int_o^\infty dv \, v^2 \int_o^h d\lambda/[h(1-\lambda/h)^{1/2}] \quad . \tag{29}$$

Circulating particles correspond to $0 \leq \lambda \leq h_m$ and trapped particles to $h_m < \lambda \leq h(\theta)$ at a given θ, where $h_m \equiv \text{MIN}[h(\theta)]$. If we further assume that $\langle\omega_{de}\rangle \simeq \hat{\omega}_{de}(v/v_e)^2$ for trapped electrons, where the pitch angle dependence has been neglected, we then find that the electron velocity integrals can be reduced to

$$U_1 = \frac{1}{2}\left(\frac{\omega-\omega_{*e}}{\omega}\right)C_1 \quad ,$$

$$U_2 = -\frac{3}{4}\left|\frac{k_\perp T_e}{eB}\right|\left(\frac{\omega-\omega_{*e}(1+\eta_e)}{\omega}\right)C_2 \quad ,$$

$$U_3 = \frac{3}{4}\left(\frac{\omega-\omega_{*e}(1+\eta_e)}{\omega}\right)\left[\left(\frac{\omega_{Be}}{\omega}\right)\frac{C_2}{2} + \left(\frac{\omega_{\kappa e}}{\omega}\right)(C_1-C_2)\right] \quad ,$$

$$T_1 = S_1 R_1 \quad ,$$

$$T_2 = -\left|\frac{k_\perp T_e}{eB}\right| S_2 R_2 \quad ,$$

$$T_3 = \left|\frac{k_\perp T_e}{eB}\right|^2 S_3 R_3 \quad ,$$

$$T_4 = S_2\left[\left(\frac{\omega_{Be}}{\omega}\right)\frac{R_2}{2} + \left(\frac{\omega_{\kappa e}}{\omega}\right)(R_1 - R_2) - \left(\frac{\hat{\omega}_{de}}{\omega}\right)R_1\right] \quad ,$$

$$T_5 = -\left|\frac{k_\perp T_e}{eB}\right| S_3\left[\left(\frac{\omega_{Be}}{\omega}\right)\frac{R_3}{2} + \left(\frac{\omega_{\kappa e}}{\omega}\right)(R_2 - R_3) - \left(\frac{\hat{\omega}_{de}}{\omega}\right)R_2\right] \quad , \qquad (30)$$

where

$$R_1 = 2(1 - h_m/h)^{1/2} \quad ,$$

$$R_2 = (4/3)(1+h_m/2h)(1-h_m/h)^{1/2} \quad ,$$

$$R_3 = \frac{16}{15}\left[1 + \frac{h_m}{2h} + \frac{3}{8}\left(\frac{h_m}{h}\right)^2\right]\left(1 - \frac{h_m}{h}\right)^{1/2} \quad ,$$

$$C_1 = 2 - R_1 \quad ,$$

$$C_2 = \frac{3}{4} - R_2 \quad ,$$

$$C_3 = \frac{16}{15} - R_3 \quad ,$$

$$S_1 = \frac{1}{2}\xi_*^2\,\eta_e - \{\xi^2 - \xi_*^2[1+\eta_e(\xi^2 - 3/2)]\}[1+\xi Z(\xi)] \quad ,$$

$$S_2 = \xi^2 S_1 - \frac{1}{2}(\xi^2 - \xi_*^2) \quad ,$$

$$S_3 = \xi^2 - \frac{3}{4}[\xi^2 - \xi_*^2(1+\eta_e)] \quad ,$$

$$\xi^2 = \omega/\hat{\omega}_{de} \quad ,$$

$$\xi_*^2 = \omega_{*e}/\hat{\omega}_{de} \quad ,$$

and Z is the plasma dispersion function.

The ion parallel velocity space integration can be carried out and the integrals are simplified to one dimensional ones, which can then be numerically integrated. These integrals can be expressed as

$$I_1 = \tau \int_0^\infty dx \exp(-x) J_{0i}^2 W \quad ,$$

$$I_2 = \tau\left(\frac{v_i}{c}\right) \int_0^\infty dx \exp(-x) J_{0i} J_{1i} \sqrt{x}\, W \quad ,$$

$$I_3 = \tau\left(\frac{v_i}{c}\right)^2 \int_0^\infty dx \exp(-x) J_{1i}^2 \tau W \quad , \qquad (31)$$

where

$$W = b[1+\xi Z(\xi)] + (a+bx) Z(\xi)/\xi \quad ,$$

$$a = -\tau[\omega - \omega_{*i}(1-3\eta_i/2)]/\omega_{\kappa i} \quad ,$$

$$b = -\omega_{*e}\eta_i/\omega_{\kappa i} \quad ,$$

$\xi^2 = -[\omega_{Bi}(x/2) - \omega]/\omega_{Ki}$, and the argument of the ion Bessel functions is $(b_i x)^{1/2}$, where $b_i = k_\perp^2 \rho_i^2$, $\rho_i = v_i/\Omega_i$. Note that the proper analytic continuation of ξ must be carried out.

Equations (26) - (28), (30) and (31) form a single second order differential equation describing the high-n collisionless ballooning modes in axisymmetric toroidal plasmas and can be solved as an eigenvalue problem for ω under the boundary condition that $\phi_\parallel$ be square integrable and $(\partial\phi_\parallel/\partial\theta)\big|_{\theta=0} = 0$. We shall solve these equations by a numerical shooting method and the results will be described in Sec. V.

In order to consider the MHD limit of Eqs. (26), (27), and (28), we neglect the trapped electron effects, which is of order $(r/R)^{1/2}$. We also take the limits $\omega_{di}/\omega \ll 1$ and $k_\perp \rho_i \ll 1$ and eliminate the ion magnetic drift resonance effect. Then the kinetic Eqs. (26) - (28) reduce to FLR modified MHD ballooning mode equation,

$$\left[\frac{1}{\partial\theta}\frac{\partial}{\partial\theta}\frac{(\nabla S)^2}{B^2}\frac{\partial}{\partial\theta} + \frac{1}{V_A^2}(\nabla S)^2\omega^2\alpha_{1i} + 8\pi K_w p' - 4\pi N T_i K_w^2 Q\right]\phi_\parallel = 0 \quad , \tag{32}$$

where $V_A^2 = B^2/4\pi N m_i$, $\omega_{*pi} = \omega_{*i}(1+\eta_i)$, $K_w = \underset{\sim}{\kappa}\cdot\hat{e}_b \times \nabla S/B$, $p' = \partial p/\partial\psi$, $p = N(T_e + T_i)$, $\underset{\sim}{\kappa} = \hat{e}_b\cdot\nabla\hat{e}_b$, $Q = 7\alpha_{2i} + 4\tau\alpha_{1i}^2/\alpha_{oe}$, and $\alpha_{\ell j} = 1 - (1+\ell\eta_j)\omega_{*j}/\omega$. Note that the K_w^2 term is of order ε_n smaller than the K_w term. For ω to be of order $(1+\eta_i)\omega_{*i}$, the K_w^2 term is destabilizing. For large aspect ratio toroidal plasmas, the K_ω^2 term in Eq. (32) is usually neglected to simulate the FLR stabilization of the ballooning modes and we will refer to this simplification as MI-1 model in the following. In addition, if we take the limit $\omega_*/\omega \to 0$, Eq. (32) reduces to the ideal MHD equation for studying infinite-n ballooning modes.

$$\left(\frac{1}{\partial\theta}\frac{\partial}{\partial\theta}\frac{(\nabla S)^2}{B^2}\frac{\partial}{\partial\theta}+\frac{(\nabla S)^2}{V_A^2}\omega^2+8\pi K_w p'\right)\psi_\parallel = 0 \quad . \tag{33}$$

In the next section we present the numerical solutions of the kinetic Eqs. (26), (27), and (28), and compare these results with those obtained from solving Eqs. (32) and (33) in order to establish the degree of validity of the simplified models (MI, MII, and ideal MHD model). There is an interesting limiting case of Eqs. (26) - (28) at $\eta_i = 0$ and without trapped particle effects. By letting $\omega = \omega_{*i}$, we find $\phi = \psi_\parallel$ from Eq. (26) and $\psi_i = -U_2\psi_\parallel/k_\perp^2\lambda_e^2$ from Eq. (27). Equation (28) then reduces to the ideal MHD equation, Eq. (33), at critical β with $\omega = 0$. This means that the critical β obtained from the kinetic Eqs. (26) - (28) is identical to the ideal MHD β_c. This observation also serves as a good way of checking the numerical solutions. For $\eta_i \neq 0$ or including trapped particle effects, we must rely on numerical solutions.

V. RESULTS

In general, we must obtain a numerical equilibrium by solving the Grad-Shafranov equation, Eq. (5), in order to integrate the eigenmode equations. However, because one of our purposes is to establish the correlations between the kinetic model and the simplified models, we will employ an analytic model equilibrium used in a number of previous ballooning mode calculations [11-13]. The model corresponds to a large aspect ratio tokamak with circular magnetic surfaces over which the poloidal magnetic field is uniform but the shear is nonuniform. Then, Eqs. (26) - (28) reduce to

$$\frac{\partial}{\partial\theta}\left[1+(\hat{s}\theta-\alpha_p\sin\theta)^2\right]\frac{\partial}{\partial\theta}\psi_\parallel = \left(\frac{\omega^2}{\frac{1}{2}\omega_A^2 b_\theta}\right)K\psi_\parallel \quad , \tag{34}$$

where

$$K = [U_1(\phi-\psi_\parallel) + U_3\psi_\parallel + T_4\phi + (U_2 + T_5)\psi_\perp]/\psi_\parallel \quad ,$$

$$\phi = [(k_\perp^2\lambda_e^2 + T_3 + I_3)U_1 - (T_2 + I_2)U_2]\psi_\parallel/D \quad ,$$

$$\psi_\perp = -[(T_2 + I_2)U_1 + (1 + \tau - T_1 - I_1)U_2]\psi_\parallel/D \quad ,$$

$$D = (1 + \tau - T_1 - I_1)(k_\perp^2\lambda_e^2 + T_3 + I_3) + (T_2 + I_2^2) \quad ,$$

$$\omega_{\kappa e} = 2\omega_{*e}\epsilon_n[\cos\theta + (\hat{s}\theta - \alpha_p \sin\theta)\sin\theta] \quad ,$$

$$\omega_{Be} = \omega_{\kappa e} - \omega_{*e}[\beta_e(1 + \eta_e) + \beta_i(1 + \eta_i)] \quad ,$$

$$\hat{\omega}_{de} = \omega_{*e}\epsilon_n \quad ,$$

$$k_\perp^2\rho_i^2 = (2b_\theta/\tau)[1 + (\hat{s}\theta - \alpha_p \sin\theta)^2] \quad , \quad \hat{s} = rq'/q \quad ,$$

$$\alpha_p = -2p'Rq^2/B^2 = (q^2/\epsilon_n)[\beta_e(1 + \eta_e) + \beta_i(1 + \eta_i)] \quad ,$$

$$\beta_e = 8\pi NT_e/B^2 \quad , \quad \beta_i = \beta_e/\tau \quad , \quad \beta = \beta_e + \beta_i \quad , \quad b_\theta = \tau k_\theta^2\rho_i^2/2 \quad ,$$

$$k_\theta = nq/r, \quad \omega_A = V_A/qR,$$

and the I's, T's, and U's are given by Eqs. (30) and (31).

Equation (32) (MI model) reduces to [10]

$$\frac{\partial}{\partial\theta}\left[1+(\hat{s}\theta-\alpha_p\sin\theta)^2\right]\frac{\partial}{\partial\theta}\phi_\parallel+\alpha_p\{[\cos\theta+(\hat{s}\theta-\alpha_p\sin\theta)\sin\theta]$$

$$+\left(\Lambda/4\right)\Omega[\Omega+(1+\eta_i)/\tau]\left[1+(\hat{s}\theta-\alpha_p\sin\theta)^2\right]$$

$$-\frac{\beta_i q^2}{2\alpha_p}\left(7\alpha_{2i}+4\tau\frac{\alpha_{1i}^2}{\alpha_{oe}}\right)[\cos\theta+(\hat{s}\theta-\alpha_p\sin\theta)\sin\theta]^2\}\phi_\parallel=0\quad,\qquad(35)$$

where $\Omega=\omega/\omega_{*e}$, $\Lambda=b_\theta/\varepsilon_p$, and $\varepsilon_p=(\varepsilon_n/2)[1+\eta_e+(1+\eta_i)/\tau]$. In Eq. (35) the eigenfrequency, Ω, is a function of the parameters, $\hat{s}$, α_p, Λ, η_i, τ, $\beta_i q^2$. While in the MI-1 model, which is given by

$$\frac{\partial}{\partial\theta}\left[1+(\hat{s}\theta-\alpha_p\sin\theta)^2\right]\frac{\partial}{\partial\theta}\phi_\parallel+\alpha_p\{[\cos\theta+(\hat{s}\theta-\alpha_p\sin\theta)\sin\theta]$$

$$+\left(\Lambda/4\right)\Omega[\Omega+(1+\eta_i)/\tau]\left[1+(\hat{s}\theta-\alpha_p\sin\theta)^2\right]\}\phi_\parallel=0\quad,\qquad(36)$$

Ω depends on the parameters $\hat{s}$, α_p, Λ, $(1+\eta_i)/\tau$ and marginal stability occurs at $\Omega=(1+\eta_i)/2\tau$. The corresonding ideal MHD ballooning model is given by

$$\frac{\partial}{\partial\theta}\left[1+(\hat{s}\theta-\alpha_p\sin\theta)^2\right]\frac{\partial}{\partial\theta}\phi_\parallel+\alpha_p[[\cos\theta+(\hat{s}\theta-\alpha_p\sin\theta)\sin\theta]$$

$$+\left(\frac{\Lambda}{4}\right)\Omega^2\left[1+(\hat{s}\theta-\alpha_p\sin\theta)^2\right]\}\phi_\parallel=0\quad,\qquad(37)$$

where Ω is a function of $\hat{s}$, α_p, and Λ only and marginal stability occurs at $\Omega=0$.

We first compare the results of the simplified models by solving Eqs. (35), (36), and (37). Figure 1 shows the growth rates and the real

frequencies versus α_p for the parameters: $\hat{s} = 0.5$, $b_\theta = 0.1$, $\varepsilon_n = 0.2$, $\tau = q = \eta_e = \eta_i = 1$. For the ideal MHD model, the growth rate is normalized by ω_{*e} defined at $b_\theta = 0.1$ and the unstable region lies between $\alpha_{p1} = 0.389$ and $\alpha_{p2} = 1.684$. The MI-1 model, Eq. (36), gives constant frequencies with $\omega_r = \omega_{*i}(1+\eta_i)/2$ when the modes are unstable and the FLR stabilization is shown by the smaller growth rates and smaller unstable region bounded by $\alpha_{p1} = 0.4843$ and $\alpha_{p2} = 1.456$. If the K_w^2 term is retained, the MI model, Eq. (35), predicts a larger unstable region than the ideal MHD model. The real frequencies are more negative. This is because for $\varepsilon_n = 0.2$, the K_w^2 term is not negligible in comparison with the K_w term and it may be incorrect to employ the MI-1 model to simulate the FLR effects.

Since the MI model is strictly valid only in the limits $b_\theta \ll 1$ and $\varepsilon_n \ll 1$, their results must be justified by comparing with the kinetic model, Eq. (34). We first neglect the trapped particle effects by setting $\varepsilon_o = 0$ and vary both b_θ and ε_n, but hold Λ fixed, from small numbers to normal tokamak values. The results are illustrated by two sets of b_θ and ε_n values ($b_\theta = \varepsilon_n = 0.01$ and $b_\theta = \varepsilon_n = 0.1$) with the eigenfrequencies versus α_p plotted in Fig. 2. The fixed parameters are $\hat{s} = 0.5$, $q = \tau = 1$, $\eta_e = \eta_i = \varepsilon_o = 0$. For $b_\theta = \varepsilon_n = 0.01$, the MI model is a good approximation of the kinetic equation when the growth rates of the modes are large. However, when the MI model predicts stable modes, the kinetic equation, Eq. (34), gives rise to small residual growth associated with the ion magnetic drift resonances. The real frequencies deviate sharply from $\omega_{*i}/2$ and reach ω_{*i} when the modes become marginally stable at the same critical β as predicted in the ideal MHD model. As b_θ and ε_n increase ($\varepsilon_n = b_\theta = 0.1$), both the growth rates and the real frequencies

from the kinetic model further deviate from those obtained by the MI models. But the stability boundaries remain the same as the ideal MHD stability boundaries in the $\eta_i = 0$ case. This larger discrepancy at larger b_θ and ε_n is due to the breakdown of the expansion in $k_\perp \rho_i$ and ω_{di}/ω as well as the omission of the magnetic drift resonances. When $\eta_i \neq 0$ the region of instability is usually greater than in the corresponding ideal MHD and MI cases.

From the parallel Ampere's law, Eq. (28), we realize that the parallel current perturbation is mainly due to circulating electrons because the trapped electron contribution is almost averaged out. Especially for deeply trapped particles $\omega_{de} - \langle \omega_{de} \rangle \simeq 0$ and from Eq. (30), T_4 and T_5 almost vanish. Therefore, when particle trapping effects are retained, the destabilizing parallel current perturbations due to circulating electron is reduced. This is different from the drift wave branch where the destabilizing contribution is due to trapped particle density perturbation through dissipation effects such as magnetic drift resonances or collisions. Figure 3 shows the eigenfrequencies versus α_p for $\varepsilon_n = 0$ and $\varepsilon_n = 0.2$, and the stabilization of the particle trapping effects is clearly seen. The results of the MI model are also shown for comparison. The fixed parameters are $\hat{s} = 0.5$, $b_\theta = 0.1$, $\varepsilon_n = 0.2$, $q = \tau = \eta_e = \eta_i = 1$.

In order to check the dependence of critical β on ε_o, Fig. 4 shows $\delta\beta$ as a function of ε_o for both the first [curve (a)] and the second [curve (b)] critical beta, where $\delta\beta = \beta_c/\beta_c(\varepsilon_o=0) - 1$ for curve (a) and $\delta\beta = 1 - \beta_c/\beta_c(\varepsilon_o=0)$ for curve (b). The fixed parameters are $\varepsilon_n = b_\theta = 0.1$, $\hat{s} = 0.5$, $q = \tau = 1$, $\eta_e = \eta_i = 0$. At $\varepsilon_o = 0$, $\beta_c = 0.03914$ for curve (a) and $\beta_c = 0.1685$ for curve (b). For small ε_o,

both curves (a) and (b) are proportional to $\varepsilon_o^{1/2}$, which can be explained by local analysis. As ε_o increases, $\delta\beta$ deviates from $\varepsilon_o^{1/2}$ dependence and becomes larger.

The FLR effects have also been studied and the results are shown in Fig. 5 with $b_\theta = 9 \times 10^{-4}$, Fig. 6 with $b_\theta = 10^{-2}$, and Fig. 7 with $b_\theta = 0.16$. In these figures the eigenfrequencies are plotted against α_p and the results of the MI and ideal MHD models are also shown for comparison. The fixed parameters are $\hat{s} = 0.6$, $q = 1.414$, $\varepsilon_n = \varepsilon_o = 0.1$, $\tau = \eta_e = \eta_i = 1$. When $b_\theta \ll 1$, as in Figs. 5 and 6, the MI mdoel and the ideal MHD model give about the same growth rates, but different real frequencies. Due to trapped particle effects, the kinetic model produces smaller stability region and smaller growth rates. As b_θ increases, both the MI model and the kinetic model begin to give substantially different results from the ideal MHD model, as shown in Fig. 7 for $b_\theta = 0.16$. Now the MI model gives rise to a smaller unstable region. If b_θ is further increased, the MI model would predict complete stability ($b_\theta \gtrsim 0.25$ for this set of parameters), but the kinetic model still predicts instabilities in a smaller α_p region than the ideal MHD model. The breakdown of the MI model is obviously due to the expansion in $k_\perp \rho_i$ and ω_{di}/ω as well as the omission of the trapped particle effects.

VI. CONCLUSION

Employing the high-n ballooning mode and WKB formalism, we have derived a collisionless kinetic ballooning mode equation in an axisymmetric toroidal plasma by solving the Vlasov-Maxwell equations. The kinetic ballooning mode equation, which includes the full ion finite Larmor radius and magnetic drift effects and the trapped electron effects, is obtained in the frequency

regime $\omega_{bi}, \omega_{ti} < \omega < \omega_{be}, \omega_{te}$. In the limit of long wavelengths, $k_\perp \rho_i \ll 1$, and small ion magnetic drift frequencies, $\omega_{di}/\omega \ll 1$, the kinetic ballooning mode equation is shown to reduce to the FLR modified MHD ballooning model and the ideal MHD model in the absence of the trapped particle effects. In order to study the influence of these kinetic effects on the stability of the ballooning modes, we perform numerical solutions of the kinetic ballooning mode equation and compare the results with those from various simplified models. In the numerical calculations we employ, for simplicity, an analytic model equilibrium which corresponds to large aspect ratio tokamaks with circular magnetic surfaces over which the poloidal magnetic field is uniform but the magnetic shear is not uniform. An interesting limit has been found with $\eta_i = 0$, $\omega = \omega_{*i}$ and without the trapped particle effects. The kinetic ballooning mode equation becomes identical to the ideal MHD equation at β_c. This implies that the ion FLR and magnetic drift resonance have no effects on the critical β for $\eta_i = 0$. In general, the ion FLR effects can reduce the growth rate but do not completely stabilize the ballooning modes due to the destabilizing influence of the ion magnetic drift resonances. Our results also show that it is incorrect to simulate the FLR effects by employing the FLR modified MHD model for $(k_\theta \rho_i)^2 \gtrsim 0.1$ and $\varepsilon_n \gtrsim 0.1$. Since the parallel current perturbation is mainly due to circulating electrons, the presence of the trapped electrons reduces the circulating electron population and gives rise to stabilizing effects. For small ε_o, the change in β_c is proportional to $\varepsilon_o^{1/2}$. For typical values of ε_o, β_c can be improved by 40%.

ACKNOWLEDGMENTS

The author would like to thank Drs. R. L. Dewar, M. S. Chance, and W. M. Tang for useful discussions.

This work was supported by United States Department of Energy Contract No. DE-AC02-76-CH03073.

REFERENCES

[1] DOBROTT, D., NELSON, D. B., GREENE, J. L., GLASSER, A. H., CHANCE, M. S., FRIEMAN, E. A., Phys. Rev. Lett. 39, 943 (1977); COPPI, B., Phys. Rev. Lett. 39, 938 (1977).

[2] GLASSER, A. H., Proceedings of the Finite Beta Theory Workshop, Varenna, 1977, edited by B. Coppi and W. Sadowski, (U. S. Department of Energy, CONF-7709167, 1977), p. 55; LEE, Y. C., VAN DAM, J. W., p. 93 of the same proceedings; CONNOR, J. W., HASTIE, R. J., TAYLOR, J. B., Proc. R. Soc. Lon. A365, 1 (1979).

[3] DEWAR, R. L., MANICKAM, J., GRIMM, R. C., CHANCE, M. S., Nucl. Fusion 21, 493 (1981).

[4] CHU, M. S., CHU, C., GUEST, G., HSU, J. Y., OHKAWA, T., Phys. Rev. Lett. 41, 247 (1978).

[5] TSANG, K. T., ORNL/TM-7324 (1980).

[6] TANG, W. M., CONNOR, J. W., WHITE, R. B., Nucl. Fusion 21, 891 (1981).

[7] CHENG, C. Z., PPPL-1782 (1981).

[8] HASTIE, R. J., HESKETH, K. W., Nucl. Fusion 21, 651 (1981).

[9] ANTONSEN, T. M., LANE, B., Phys. Fluids 23, 1205 (1980).

[10] TANG, W. M., CONNOR, J. W., HASTIE, R. J., Nucl. Fusion 20, 1439 (1980).

[11] CONNOR, J. W., HASTIE, R. J., TAYLOR, J. B., Phys. Rev. Lett. 40, 396 (1978).

[12] LORTZ, D., NUHRENBERG, J., Phys. Lett. 68A, 49 (1978).

[13] POGUTSE, O. P., YURCHENKO, E. I., Sov. J. Plasma Phys. 5, 441 (1979).

[14] GRIMM, R. C., GREENE, J. M., JOHNSON, J. L., in Methods in Computational Physics, Vol. 16, J. Killeen, ed. (Academic, NY 1976) p. 253.

FIGURE CAPTIONS

Fig. 1. Dependence of the growth rates and the real frequencies on α_p for $\hat{s} = 0.5$, $b_\theta = 0.1$, $\varepsilon_n = 0.2$, $\varepsilon_o = 0$, $\tau = q = \eta_e = \eta_i = 1$ where $\alpha_p = -2p'Rq^2/B^2 = \beta q^2[1 + \eta_i + \tau(1 + \eta_e)]/[\varepsilon_n(1 + \tau)]$. The eigen frequencies obtained from the MI model [Eq. (35)], the MI-1 model [Eq. (36)], and the ideal MHD model [Eq. (37)] are compared.

Fig. 2. Plot of the eigenfrequencies versus α_p for two sets of b_θ and ε_n values: (a) $b_\theta = \varepsilon_n = 0.01$, and (b) $b_\theta = \varepsilon_n = 0.1$. The fixed parameters are $\hat{s} = 0.5$, $q = \tau = 1$, $\eta_e = \eta_i = \varepsilon_o = 0$. The results from the kinetic model, Eq. (34), the MI model, Eq. (35), and the ideal MHD model, Eq. (37), are compared.

Fig. 3. Dependence of the eigenfrequencies from the kinetic model, Eq. (34), on α_p for two values of ε_o: $\varepsilon_o = 0$ and $\varepsilon_o = 0.2$. The fixed parameters are $\hat{s} = 0.5$, $b_\theta = 0.1$, $\varepsilon_n = .2$, $q = \tau = \eta_e = \eta_i = 1$. The results of the MI model, Eq. (35), are also shown for comparison.

Fig. 4. Dependence of $\delta\beta$ on ε_o for both the first [curve (a)] and the second [curve (b)] critical β, where $\delta\beta = \beta_c/\beta_c(\varepsilon_o = 0) - 1$ for curve (a) and $\delta\beta = 1 - \beta_c/\beta_c(\varepsilon_o = 0)$ for curve (b). At $\varepsilon_o = 0$, $\beta_c = 0.03914$ for curve (a) and $\beta_c = 0.1685$ for curve (b). The fixed parameters are $\varepsilon_n = b_\theta = 0.1$, $\hat{s} = 0.5$, $q = \tau = 1$, $\eta_e = \eta_i = 0$.

Fig. 5. Dependence of the eigenfrequencies from the kinetic model, Eq. (34), the MI model, Eq. (35), and the ideal MHD model, Eq. (37), on α_p for $b_\theta = 9 \times 10^{-4}$. The fixed parameters are $\hat{s} = 0.6$, $q = 1.414$, $\varepsilon_o = \varepsilon_n = 0.1$, $\tau = \eta_e = \eta_i = 1$.

Fig. 6. Same as in Fig. 5 except $b_\theta = 0.01$.

Fig. 7. Same as in Fig. 5 except $b_\theta = 0.16$.

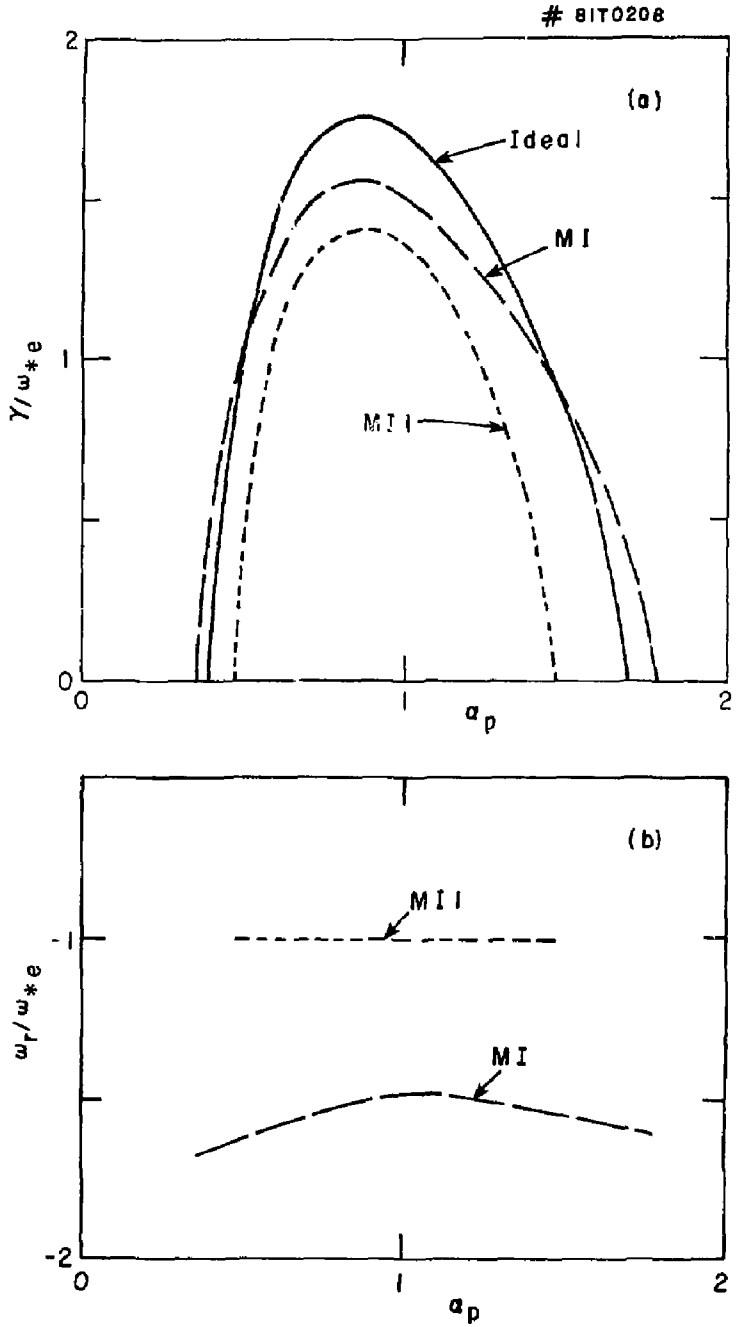
81T0208
(a)
Ideal
MI
MII
γ/ω_{*e}
2
1
0
0
1
2
a_p
(b)
MII
MI
ω_r/ω_{*e}
-1
-2
0
1
2
a_p

Fig. 1

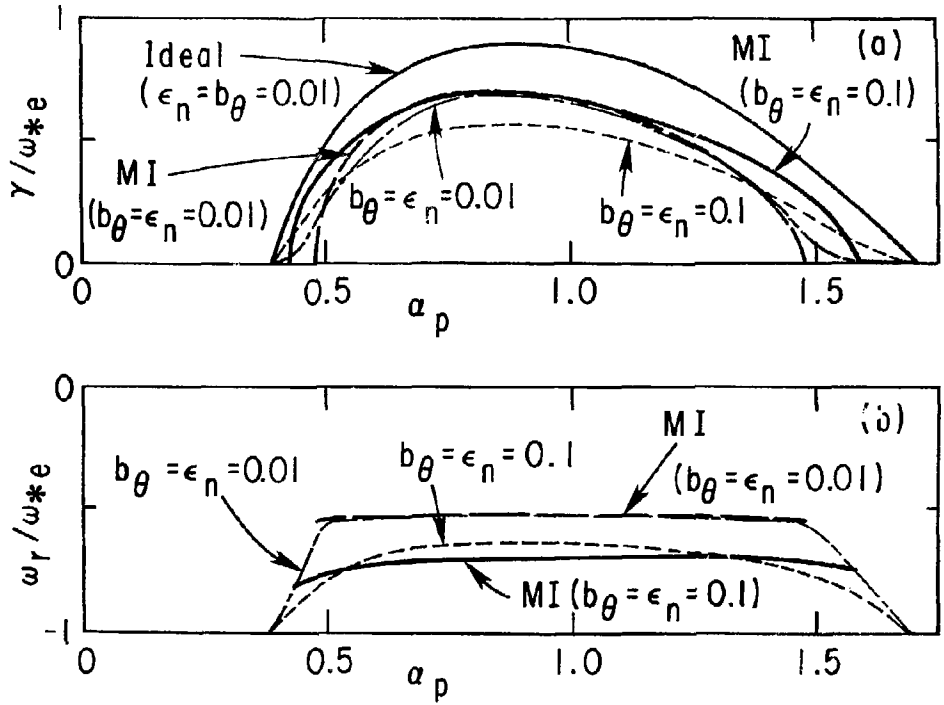
Ideal
($\epsilon_n = b_\theta = 0.01$)
MI
($b_\theta = \epsilon_n = 0.01$)
$b_\theta = \epsilon_n = 0.01$
$b_\theta = \epsilon_n = 0.1$
MI
($b_\theta = \epsilon_n = 0.1$)
(a)
γ / ω_{*e}
α_p
0
0.5
1.0
1.5
$b_\theta = \epsilon_n = 0.01$
$b_\theta = \epsilon_n = 0.1$
MI
($b_\theta = \epsilon_n = 0.01$)
MI ($b_\theta = \epsilon_n = 0.1$)
(b)
ω_r / ω_{*e}
-1

Fig. 2

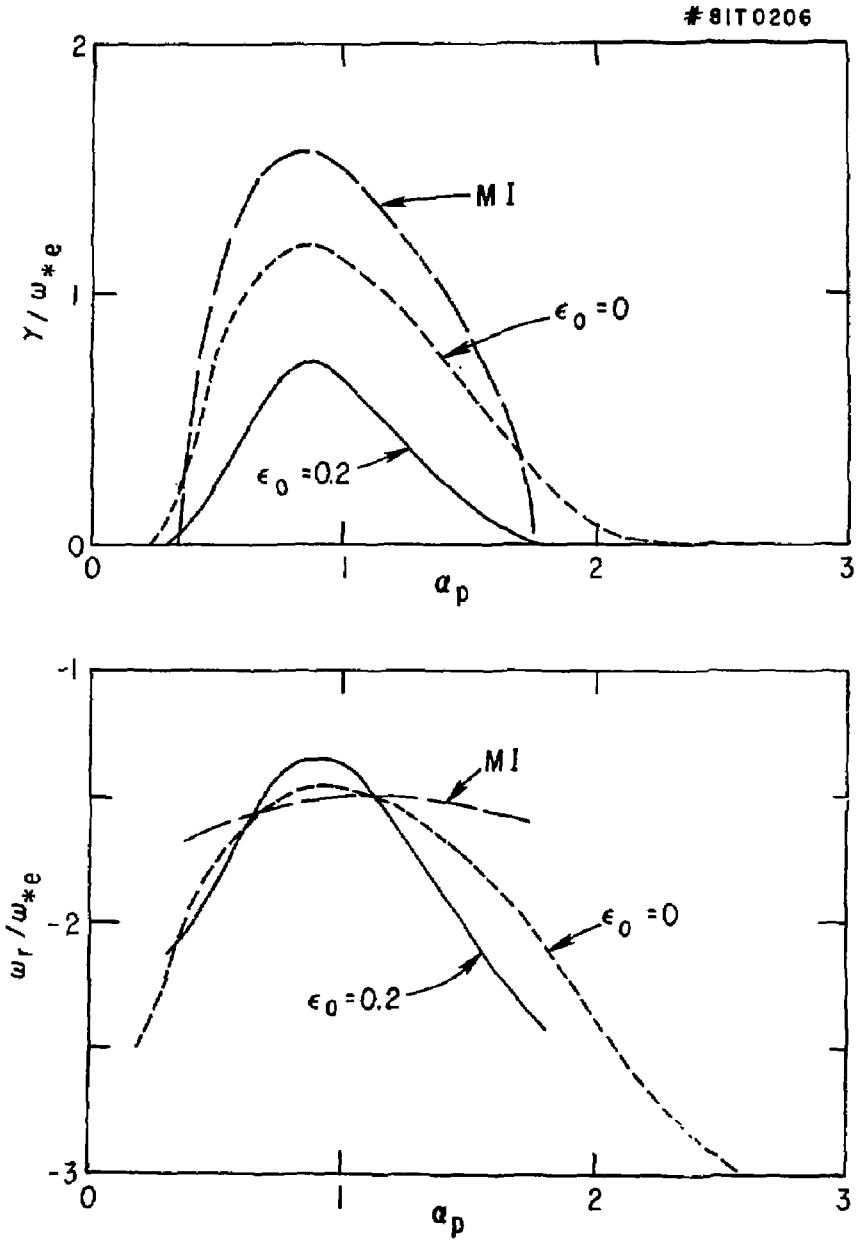
#81T0206
2
1
0
γ / ω_{*e}
MI
$\epsilon_0 = 0$
$\epsilon_0 = 0.2$
0
1
2
3
α_p
-1
-2
-3
ω_r / ω_{*e}
MI
$\epsilon_0 = 0$
$\epsilon_0 = 0.2$
0
1
2
3
α_p

Fig. 3

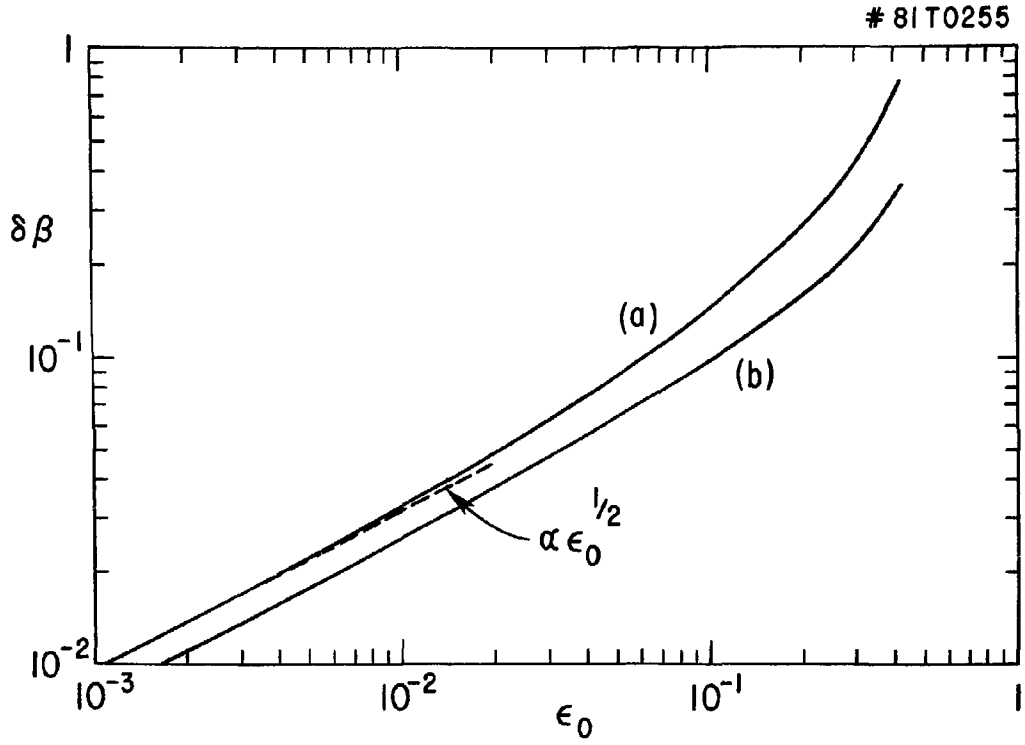
81T0255
1
$\delta\beta$
10^{-1}
10^{-2}
10^{-3}
10^{-2}
10^{-1}
1
ϵ_0
(a)
(b)
$\propto \epsilon_0^{1/2}$

Fig. 4

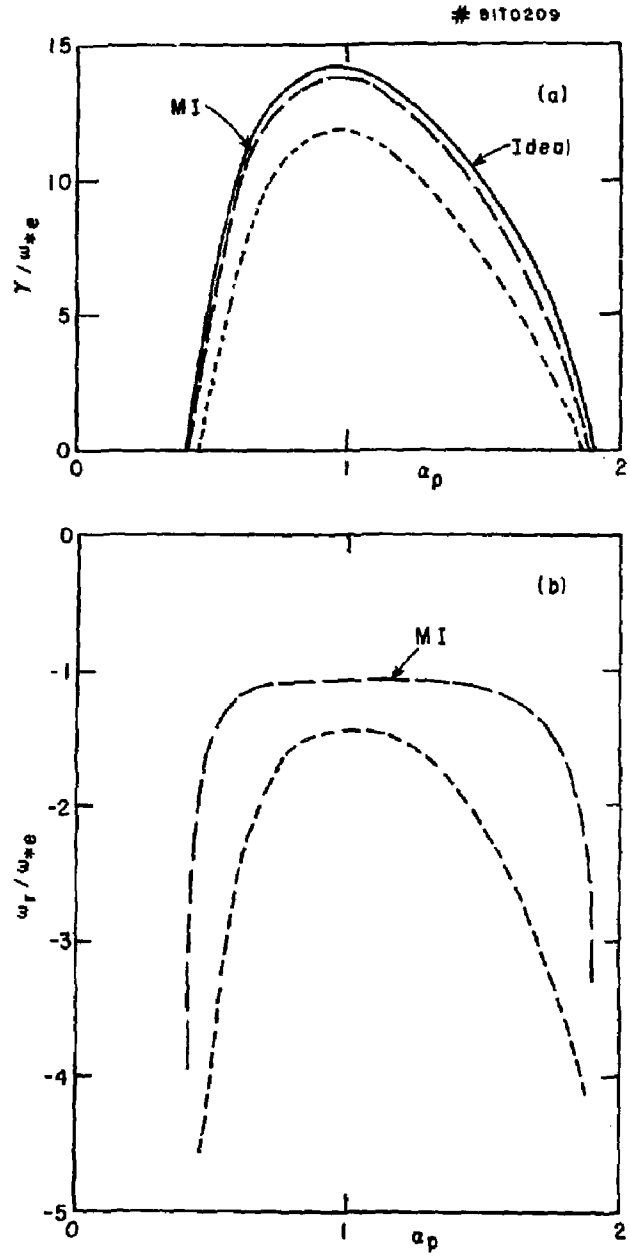
* 81T0209
(a)
MI
Ideal
γ / ω_{*e}
α_p
(b)
MI
ω_r / ω_{*e}
α_p

Fig. 5

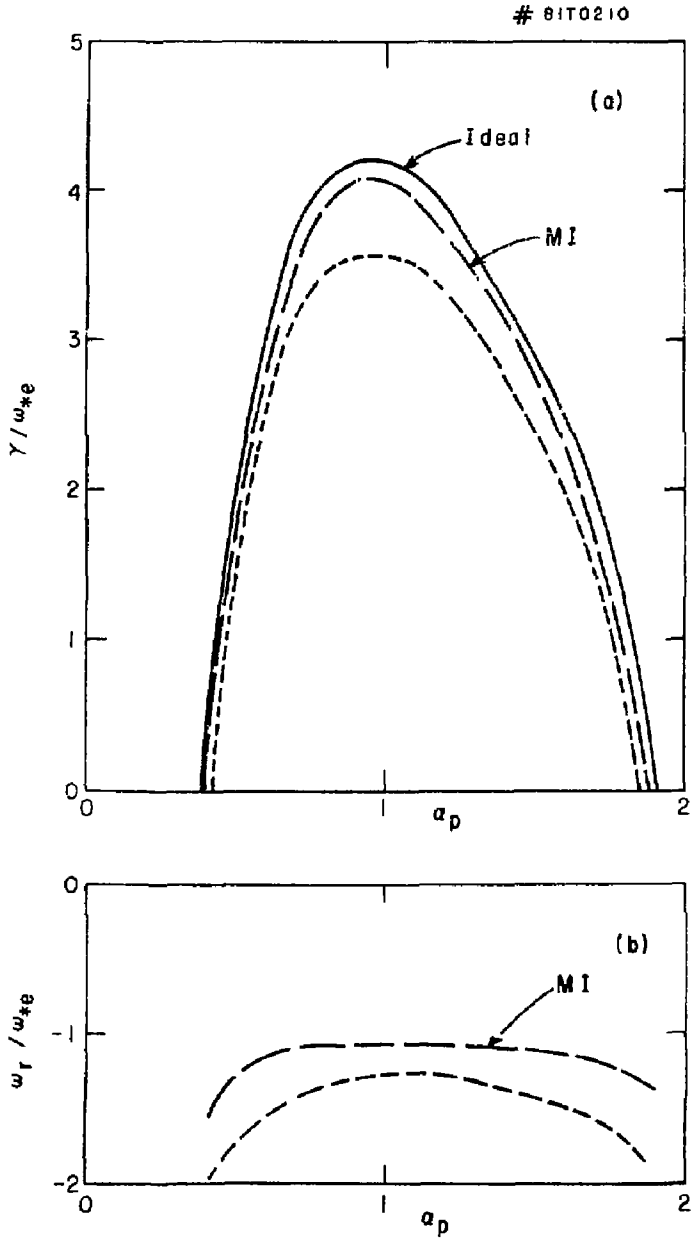
81T0210
(a)
Ideal
MI
γ / ω_{*e}
α_p
(b)
MI
ω_r / ω_{*e}
α_p

Fig. 6

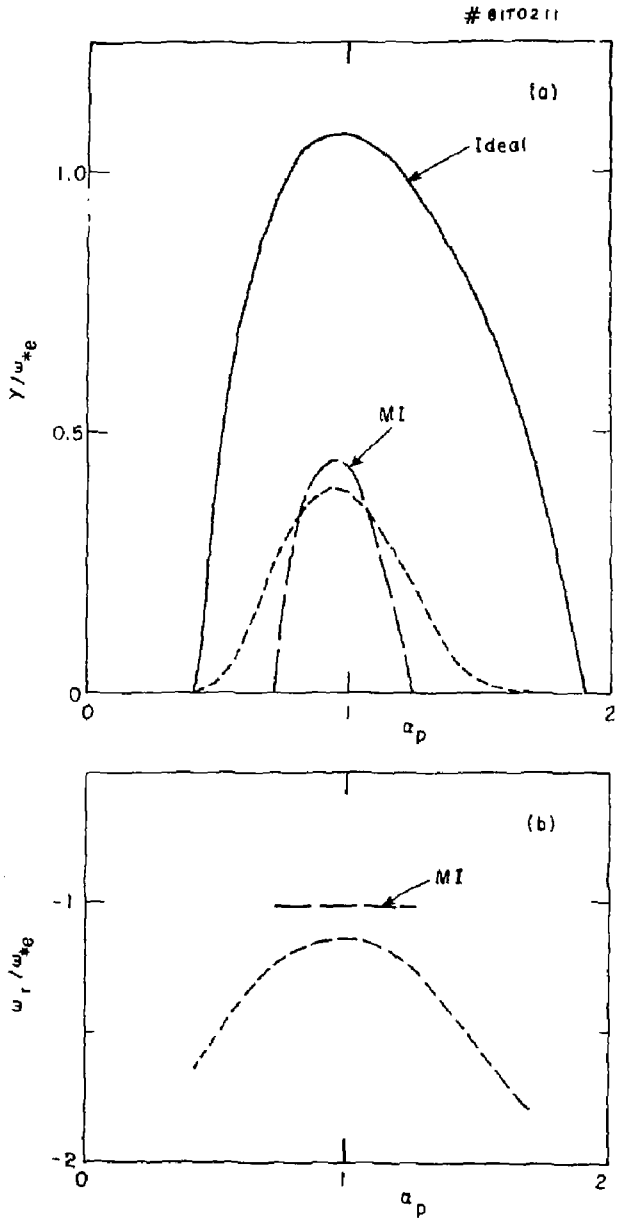
#81T021
(a)
Ideal
MI
1.0
0.5
0
γ/ω_{*e}
0
1
2
α_p
(b)
MI
-1
-2
ω_r/ω_{*e}
0
1
2
α_p

Fig. 7